

Engineering Notes

ENGINEERING NOTES are short manuscripts describing new developments or important results of a preliminary nature. These Notes cannot exceed 6 manuscript pages and 3 figures; a page of text may be substituted for a figure and vice versa. After informal review by the editors, they may be published within a few months of the date of receipt. Style requirements are the same as for regular contributions (see inside back cover).

Optimal Orbital Transfer with Electrodynamic Tether

Paul Williams*

RMIT University, Melbourne, Victoria 3083, Australia

Introduction

ELECTRODYNAMIC tethers provide an efficient means for performing orbital transfers. In particular, the relatively new propellantless technology allows systems to be transferred from one orbit to another by simply modulating the level of electric current in the long, conducting tether. Because the tether is traveling through the Earth's magnetic field at high velocity, an electromotive force is generated that can alter the spacecraft's orbit. However, the force generated in the tether is a vector product of the Earth's magnetic field and the local direction of the conducting tether, which generates a Lorentz force perpendicular to both the tether and the magnetic field. This means that careful control of the current is necessary to effect desired changes to the spacecraft orbit.

Various studies have been undertaken on the use of electrodynamic tethers to perform orbit transfers. For example, Johnson and Herrmann¹ and Vas et al.² considered reboosting the orbit of the International Space Station using electrodynamic tethers. Hoyt and Forward³ designed the terminator tether system, which is capable of autonomously deorbiting small satellites. Lanoix et al.⁴ studied the influence of electromagnetic forces on the orbital motion of tethered satellites and considered a very simple control scheme to alleviate the buildup of large-amplitude tether librations. Similarly, Hoyt⁵ has introduced feedback control to keep the tether librations within suitably selected bounds. More recently, Tragesser and San⁶ designed a guidance control methodology to transfer an electrodynamic tether system between selected orbits. However, it was assumed that the tether remains pointed along the local vertical (i.e., there are no tether librations), and bounds on the control current were not explicitly enforced. The control methodology used by Tragesser and San is based on the linear combination of current controls necessary to yield secular changes in each of the orbital elements.

In this Note, the work of Tragesser and San⁶ is extended within the scope of orbit boost and deboost to consider optimal orbital maneuvers. Most important, in this work the tether librations are explicitly accounted for when determining the optimal control input, together with suitable bounds on the control. In addition, no assumption about the variation in the control current is made. The effect of the tether librations on the performance of the orbit maneuvers is also considered by 1) determining the optimal control input with the tether assumed to remain along the local vertical and

2) comparing the results with the full dynamic interaction of tether librations. The complex optimal control problem is solved using a direct transcription approach.

Equations of Motion

The electric current flowing within the tether is generally restricted to relatively small magnitudes that depend on the density of the ionospheric plasma and several properties of the tether system. The electromagnetic force generated by the system is therefore relatively small and the system behaves in some ways like a low-thrust spacecraft. The most fundamental difference between electrodynamic-driven and conventional low-thrust spacecraft is that the electromagnetic force can be generated only in a direction normal to both the tether and the local magnetic field. Therefore, transferring an electrodynamic tether system from one orbit to another cannot be achieved in a straightforward manner. Because the orbital elements are expected to change slowly, it is much more convenient to express the motion of the system using orbital perturbation equations. For simplicity, a set of classical orbital parameters are used rather than a set of modified equinoctial elements. The classical perturbation equations become ill-conditioned for vanishing eccentricities, however, and future work would need to consider more general equations than those considered here.

The Gauss form of the variational equations is given by⁷

$$\dot{a} = (2a^2/h)[e \sin(v) f_r + (p/r) f_\theta] \quad (1)$$

$$\dot{e} = (1/h)\{p \sin(v) f_r + [(p+r) \cos v + re] f_\theta\} \quad (2)$$

$$\dot{i} = (r \cos(\omega + v)/h) f_h \quad (3)$$

$$\dot{\Omega} = (r \sin(\omega + v)/h \sin i) f_h \quad (4)$$

$$\dot{\omega} = (1/he)[-p \cos(v) f_r + (p+r) \sin(v) f_\theta - [r \sin(\omega + v) \cos i / h \sin i] f_h] \quad (5)$$

$$\dot{v} = h/r^2 + (1/eh)[p \cos(v) f_r - (p+r) \sin(v) f_\theta] \quad (6)$$

where a is the orbit semimajor axis; $h = \sqrt{\mu a(1-e^2)}$ is the orbit angular momentum; v is the orbit true anomaly; ω is the argument of perigee; $p = a(1-e^2)$ is the semi-latus rectum; $r = p/(1+e \cos v)$ is the orbit radius; e is the orbit eccentricity; Ω is the right ascension of the ascending node; i is the orbit inclination; and f_r , f_θ , and f_h are the components of the disturbing acceleration vector in the radial, transverse, and orbit normal directions, respectively.

The tether librational dynamics are governed by a set of second-order differential equations describing the in-(θ) and out-of-plane (ϕ) librational oscillations with respect to the Euler–Hill orbital frame:

$$\ddot{\theta} = -\ddot{v} + 2(\dot{\theta} + \dot{v})\dot{\phi} \tan \phi - 3[\dot{v}^2/(1+e \cos v)] \sin \theta \cos \theta + Q_\theta / m^* L^2 \cos^2 \phi \quad (7)$$

$$\ddot{\phi} = -\{(\dot{\theta} + \dot{v})^2 + 3[\dot{v}^2/(1+e \cos v)] \cos^2 \theta\} \sin \phi \cos \phi + Q_\phi / m^* L^2 \quad (8)$$

where Q_θ and Q_ϕ are the electromagnetic torques on the tether system, L is the tether length, $m^* = (m_1 + m_t/2)(m_2 + m_t/2)/m -$

Received 5 July 2004; revision received 17 August 2004; accepted for publication 6 October 2004. Copyright © 2004 by Paul Williams. Published by the American Institute of Aeronautics and Astronautics, Inc., with permission. Copies of this paper may be made for personal or internal use, on condition that the copier pay the \$10.00 per-copy fee to the Copyright Clearance Center, Inc., 222 Rosewood Drive, Danvers, MA 01923; include the code 0731-5090/05 \$10.00 in correspondence with the CCC.

*Research Fellow, School of Aerospace, Mechanical, and Manufacturing Engineering. Student Member AIAA.

$m_t/6$ is the reduced system mass, m_1 and m_2 are the subsatellite masses, m_t is the tether mass, and m is the total system mass.

Electromagnetic Forces

The electromagnetic force acting on an element of tether is given by

$$d\mathbf{F} = I d\mathbf{l} \times \mathbf{B} \quad (9)$$

where $d\mathbf{l}$ is a vector tangential to the tether line, I is the current in the tether, and \mathbf{B} is the Earth's magnetic field vector in the Euler–Hill frame whose components are defined by (assuming a nontilted dipole)

$$B_x = -2(\mu_m/R^3) \sin(\omega + \nu) \sin i \quad (10)$$

$$B_y = (\mu_m/R^3) \cos(\omega + \nu) \sin i \quad (11)$$

$$B_z = (\mu_m/R^3) \cos i \quad (12)$$

The electromagnetic torques on the tether may be determined by integrating Eq. (9) along the tether and using the principle of virtual work:

$$Q_\theta = (IL^2/2)\Theta \cos \phi [\sin \phi (B_x \cos \theta + B_y \sin \theta) - B_z \cos \phi] \quad (13)$$

$$Q_\phi = -(IL^2/2)\Theta [B_y \cos \theta - B_x \sin \theta] \quad (14)$$

where $\Theta = [m_1^2 - m_2^2 + m_t(m_1 - m_2)]/m^2$ is the nondimensional parameter that defines a measure of the average moment arm of the electromagnetic torque acting on the tether relative to the system center of mass. Note that this assumes a uniform current flowing in the tether. In the case where the mass distribution is perfectly symmetrical, then the net torque about the center of mass is zero. This is an ideal scenario that is unlikely to be achieved in practice. This effect will still be present in bare-wire tethers, but the relationship is not as straightforward because of the nonuniform distribution of the electric current.

The perturbative accelerations due to electromagnetic forces are

$$f_r = IL/m(B_z \sin \theta \cos \phi - B_y \sin \phi) \quad (15)$$

$$f_\theta = IL/m(B_x \sin \phi - B_z \cos \theta \cos \phi) \quad (16)$$

$$f_\phi = IL/m(B_y \cos \theta \cos \phi - B_x \sin \theta \cos \phi) \quad (17)$$

Similar equations were used by Tragesser and San⁶ assuming that the tether does not librate (i.e., $\theta = \phi = 0$). For a nonlibrating tether, no force can be generated radially to assist in orbital maneuvering. However, it is clear that in the presence of three-dimensional librations the form of the perturbative force on the system is quite different from that of a radially aligned tether, and it may be possible to effectively use the librations during the orbit transfer.

Optimal Orbit Transfers

In this Note, a simple orbit transfer with parameters taken from Ref. 6 is considered. Essentially, we would like to compare the characteristics of an optimal orbit transfer with the characteristics of the maneuver considered by Tragesser and San,⁶ but with the effect of tether librations also incorporated.

We consider orbit transfers that increase the orbit semimajor axis (orbit boost) or decrease the orbit semimajor axis (deboost). By restricting the available current, we are interested in achieving efficient orbital maneuvers. For this purpose, we consider fixed-time orbit transfers. The problem is to find the current control input $I(t)$ that transfers the tether system from the initial orbit:

$$[a, e, i, \Omega, \omega, \nu]_0 = [a_0, e_0, i_0, \Omega_0, \omega_0, \nu_0] \quad (18)$$

to the orbit with maximum change in the orbit semimajor axis a with corresponding orbital parameters,

$$[e, i, \Omega, \omega]_{t_f} = [e_0, i_0, \Omega_0, \omega_0] \quad (19)$$

where the subscript 0 indicates the reference initial state.

Direct Transcription

Direct transcription is a widely used approach for solving optimal control problems.⁸ In this work, the Hermite–Simpson method⁹ is used because a large number of collocation points and a bang-bang control input are expected. These are important considerations, particularly when the sparsity of the Jacobian is taken into consideration.¹⁰ The Jacobians in other methods such as pseudospectral methods¹¹ are considerably less sparse than standard discretizations,¹⁰ making pseudospectral methods less efficient for very large problems. Direct transcription methods are routinely implemented with standard nonlinear programming (NLP) software such as SNOPT¹² or SPRNLP.¹³ In this paper, SNOPT is used as the NLP software.

The main advantage of using direct transcription methods for obtaining solutions to optimal control problems is that nonintuitive costates do not appear in the problem formulation. Because of this, direct methods do not give a straightforward way of assessing the optimality of a solution. The feasibility of the solution, however, can be checked by simply propagating the control history using a higher-order integrator, such as a Runge–Kutta scheme. In this work, a simple approach is introduced to verify the optimality of the direct solution. For autonomous problems, it is known that the minimized Hamiltonian must be constant and that the costates must satisfy certain boundary conditions. For free terminal boundary conditions on the states, the corresponding costates should be equal to zero, and for a state being maximized (or minimized) at the terminal time, the corresponding costate must be equal to ± 1 . The Lagrange multipliers provided by the NLP software give discrete approximations to the costates of the optimal control problem. Although for several discretizations the order of approximation for the costates and the states are not the same, the costates are nevertheless sufficiently accurate to test the optimality of the solution. Thus, for the Hermite–Simpson method, it is possible to construct a discrete representation of the Hamiltonian and calculate the error from optimality by determining the maximum variation in the value of the Hamiltonian. Note, however, that this approach is still unable to distinguish between local and global minima.

Numerical Results

The system parameters used for the numerical computations were selected as

$$[a_0, e_0, i_0, \Omega_0, \omega_0, \nu_0] = [6878 \text{ km}, 0.02, 30 \text{ deg}, 30 \text{ deg}, 50 \text{ deg}, 0]$$

with $m_1 = 250$ kg, $m_2 = 150$ kg, $m_t = 20$ kg, and $L = 15$ km. The time variable is nondimensionalized with respect to the mean anomaly, and the final time is fixed at $t_f = 100$ rad. This was selected because of memory limitations of the personal computer used to perform the numerical calculations. The total number of collocation points was selected as 400 (evenly spaced), which gives 4400 optimization variables and 4004 equality constraints. Numerical results are obtained for the following cases: 1) maximum orbit boost with nonlibrating tether, 2) maximum orbit boost with librating tether, 3) maximum orbit deboost with nonlibrating tether, and 4) maximum orbit deboost with librating tether. The control current is limited to the range $-4 \leq I(t) \leq 4$ A, and the tether is assumed to be initially nonlibrating. Note that in general the current will be restricted by the available ionospheric plasma, rather than the strict limitations enforced here. However, more advanced constraints are beyond the scope of this Note.

Numerical results for cases 1 and 2 are shown in Fig. 1, whereas the results for cases 3 and 4 are shown in Fig. 2. These results have been propagated using ode45 in MATLAB to verify the feasibility of the direct transcription solution. The optimality of the results is verified by noting that the minimized Hamiltonian is approximately constant with maximum changes of 9.59×10^{-4} , 1.31×10^{-3} , 1.26×10^{-3} , and 9.21×10^{-4} for cases 1 to 4, respectively. Note that the minimized Hamiltonian is approximately equal to zero for this formulation of the problem. The boundary conditions on the costates were also found to be in agreement with optimal control theory. Figure 1 shows that the control current has a mean negative value but is of a bang-bang nature. This is consistent with

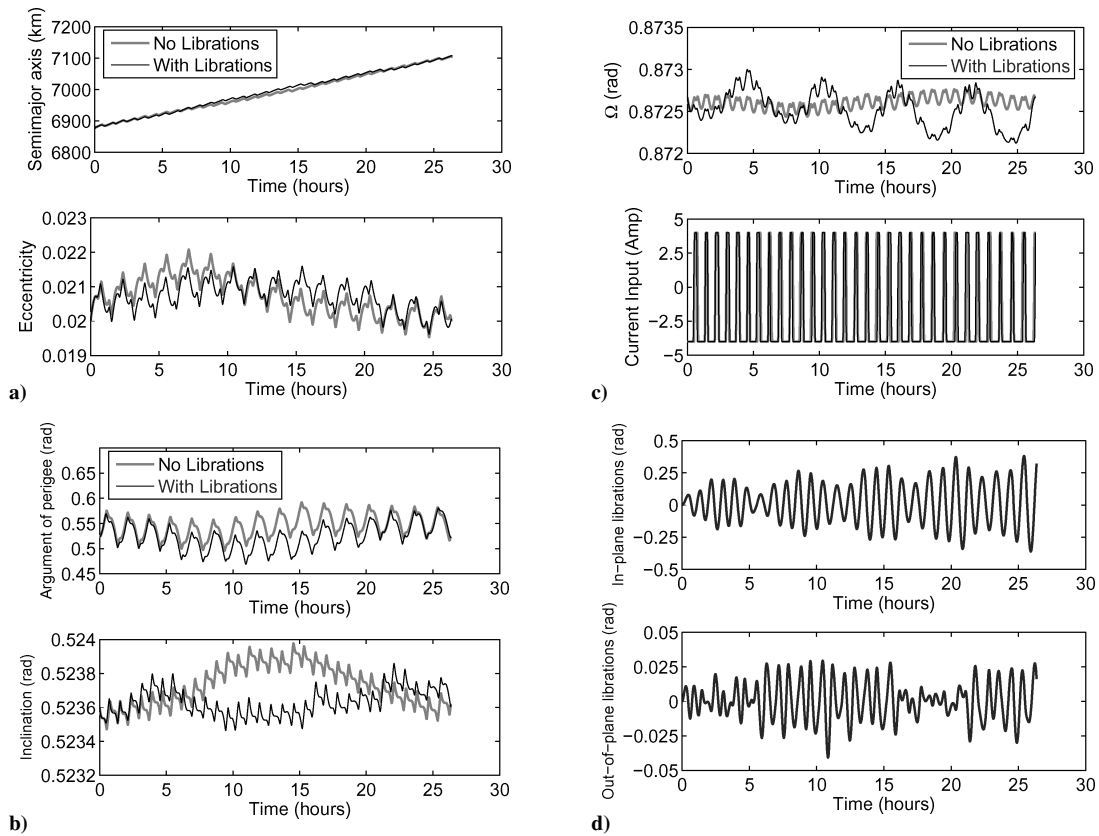


Fig. 1 Optimal orbit boost with electrodynamic tether.

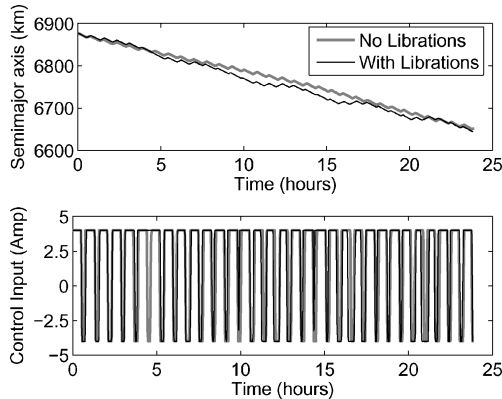


Fig. 2 Optimal orbit deboost with electrodynamic tether.

the sign conventions necessary to generate a propulsive force. The reverse is true for the deboost scenario, as shown in Fig. 2. The control current for the orbit boost case is not significantly different from the case when tether librations are included, but Fig. 2 shows that there are some differences in the control input when tether librations are considered (orbit deboost). It is also clear that the evolution of the orbital elements is quite different depending on whether tether librations are considered, particularly the orbital inclination and line of nodes. Note that the orbital elements for the deboost scenario are not presented because their variation is qualitatively similar to orbit boost. It is therefore prudent that the effect of tether librations be considered when performing orbital maneuvers with electrodynamic tethers. Furthermore, it is apparent that the optimal orbit maneuver with electrodynamic tethers does not yield secular changes in orbital elements in the same manner as those obtained by Tragesser and San.⁶

One important consequence of the inclusion of tether librations compared to the case where no librations are included is that there is an improvement in the final value of the semimajor axis. For example, for the orbit boost case, the increase in semimajor axis without librations is 226.2 km, whereas with tether librations the

increase is 229.6 km (1.5% improvement). Similarly, for the deboost case without librations, the decrease in the orbit semimajor axis is 226.1 km, whereas with tether librations the decrease is 233.3 km (3.2% improvement). The improvement is also impressive from the point of view of the difference in dimensional time required for the two maneuvers (see the scale on the independent variable). The main reason for the difference in performance is because of the effect of tether librations on the direction of the Lorentz force. Because the tether system is on an inclined orbit, the tether librations alter the orientation of the tether relative to the magnetic field, allowing larger components of the thrust or drag forces to be generated tangential to the orbit. As seen in Eq. (1), this allows more rapid changes in the orbit semimajor axis for small eccentricity orbits. It may therefore be possible to design controllers for electrodynamic tether systems that use tether librations beneficially for orbit transfer, rather than viewing the librations as an instability to keep to a minimum as has been done in previous studies.^{4,5}

Conclusions

Optimal orbit transfers using electrodynamic tethers have been considered. The orbit perturbation equations, together with the tether librational dynamics, have been used to generate optimal orbit boost and deboost trajectories in a specified time using direct transcription. It has been shown that the evolution of some of the orbital parameters are strongly affected by the tether librations. Furthermore, the tether librations can lead to improved orbit transfers compared to the case where the tether is assumed to remain vertical along the radial direction. Further work should be undertaken to assess the effect of tether lateral flexibility and longer orbit transfer times on the efficiency of orbit transfers using electrodynamic tethers.

References

- Johnson, L., and Herrmann, M., "International Space Station Electrodynamic Tether Reboost Study," NASA TM-1998-208538, 1998.
- Vas, I. E., Kelly, T. J., and Scarl, E., "Application of an Electrodynamic Tether System to Reboost the International Space Station," *Proceedings of the Tether Technology Interchange Meeting*, NASA CP-1998-206900, 1998.

³Hoyt, R. P., and Forward, R. L., "The Terminator Tether: Autonomous Deorbit of LEO Spacecraft for Space Debris Mitigation," AIAA Paper 2000-0329, Jan. 2000.

⁴Lanoix, E. L. M., Misra, A. K., Modi, V. J., and Tyc, G., "Effect of Electromagnetic Forces on the Orbital Dynamics of Tethered Satellites," *AAS/AIAA Spaceflight Mechanics Meeting*, edited by C. A. Kluever, B. Neta, C. D. Hall, and J. M. Hanson, Univelt, San Diego, CA, 2000, pp. 1347–1365.

⁵Hoyt, R. P., "Stabilization of Electrodynamic Space Tethers," *Proceedings of Space Technology and Applications International Forum (STAIF-2002)*, American Inst. of Physics, Melville, NY, 2002, pp. 570–577.

⁶Tragesser, S. G., and San, H., "Orbital Maneuvering with Electrodynamic Tethers," *Journal of Guidance, Control, and Dynamics*, Vol. 26, No. 5, 2003, pp. 805–810.

⁷Kechichian, J. A., "Trajectory Optimization Using Nonsingular Orbital Elements and True Longitude," *Journal of Guidance, Control, and Dynamics*, Vol. 20, No. 5, 1997, pp. 1003–1009.

⁸Betts, J. T., "Survey of Numerical Methods for Trajectory Optimization," *Journal of Guidance, Control, and Dynamics*, Vol. 21, No. 2, 1998, pp. 193–207.

⁹Hargraves, C. R., and Paris, S. W., "Direct Trajectory Optimization Using Nonlinear Programming and Collocation," *Journal of Guidance, Control, and Dynamics*, Vol. 10, No. 4, 1987, pp. 338–342.

¹⁰Betts, J. T., *Practical Methods for Optimal Control Using Nonlinear Programming*, Society for Industrial and Applied Mathematics, Philadelphia, 2001.

¹¹Ross, I. M., and Fahroo, F., "Pseudospectral Knotting Methods for Solving Optimal Control Problems," *Journal of Guidance, Control, and Dynamics*, Vol. 27, No. 3, 2004, pp. 397–405.

¹²Gill, P. E., Murray, W., and Saunders, M. A., "SNOPT: An SQP Algorithm for Large-Scale Constrained Optimization," *SIAM Journal of Optimization*, Vol. 12, No. 4, 2002, pp. 979–1006.

¹³Betts, J. T., and Frank, P. D., "A Sparse Nonlinear Optimization Algorithm," *Journal of Optimization Theory and Applications*, Vol. 82, No. 3, 1994, pp. 519–541.